NASA/TM–2008-215364 **TFAWS 08-1001**

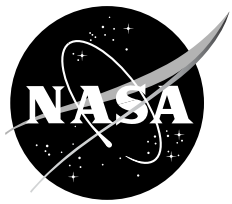

Thermal Capacitance (Slug) Calorimeter Theory Including Heat Losses and Other Decaying Processes

T. Mark Hightower and Ricardo A. Olivares
Ames Research Center, Moffett Field, California

Daniel Philippidis
San Jose State University, San Jose, California

September 2008

The NASA STI Program Office . . . in Profile

Since its founding, NASA has been dedicated to the advancement of aeronautics and space science. The NASA Scientific and Technical Information (STI) Program Office plays a key part in helping NASA maintain this important role.

The NASA STI Program Office is operated by Langley Research Center, the Lead Center for NASA's scientific and technical information. The NASA STI Program Office provides access to the NASA STI Database, the largest collection of aeronautical and space science STI in the world. The Program Office is also NASA's institutional mechanism for disseminating the results of its research and development activities. These results are published by NASA in the NASA STI Report Series, which includes the following report types:

- TECHNICAL PUBLICATION. Reports of completed research or a major significant phase of research that present the results of NASA programs and include extensive data or theoretical analysis. Includes compilations of significant scientific and technical data and information deemed to be of continuing reference value. NASA's counterpart of peer-reviewed formal professional papers but has less stringent limitations on manuscript length and extent of graphic presentations.

- TECHNICAL MEMORANDUM. Scientific and technical findings that are preliminary or of specialized interest, e.g., quick release reports, working papers, and bibliographies that contain minimal annotation. Does not contain extensive analysis.

- CONTRACTOR REPORT. Scientific and technical findings by NASA-sponsored contractors and grantees.

- CONFERENCE PUBLICATION. Collected papers from scientific and technical conferences, symposia, seminars, or other meetings sponsored or cosponsored by NASA.

- SPECIAL PUBLICATION. Scientific, technical, or historical information from NASA programs, projects, and missions, often concerned with subjects having substantial public interest.

- TECHNICAL TRANSLATION. English-language translations of foreign scientific and technical material pertinent to NASA's mission.

Specialized services that complement the STI Program Office's diverse offerings include creating custom thesauri, building customized databases, organizing and publishing research results . . . even providing videos.

For more information about the NASA STI Program Office, see the following:

- Access the NASA STI Program Home Page at *http://www.sti.nasa.gov*

- E-mail your question via the Internet to help@sti.nasa.gov

- Fax your question to the NASA Access Help Desk at (301) 621-0134

- Telephone the NASA Access Help Desk at (301) 621-0390

- Write to:
  NASA Access Help Desk
  NASA Center for AeroSpace Information
  7115 Standard Drive
  Hanover, MD 21076-1320

NASA/TM–2008-215364 **TFAWS 08-1001**

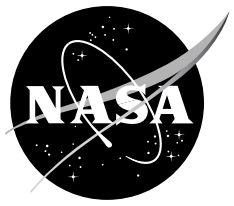

Thermal Capacitance (Slug) Calorimeter Theory Including Heat Losses and Other Decaying Processes

T. Mark Hightower and Ricardo A. Olivares
Ames Research Center, Moffett Field, California

Daniel Philippidis
San Jose State University, San Jose, California

Prepared for the
Thermal and Fluids Analysis Workshop (TFAWS) 2008
sponsored by Ames Research Center and San Jose State University
at San Jose State University, San Jose, California, August 18–22, 2008

National Aeronautics and
Space Administration

Ames Research Center
Moffett Field, California 94035-1000

September 2008

Available from:

NASA Center for AeroSpace Information
7115 Standard Drive
Hanover, MD 21076-1320
(301) 621-0390

National Technical Information Service
5285 Port Royal Road
Springfield, VA 22161
(703) 487-4650

TABLE OF CONTENTS

LIST OF FIGURES

LIST OF TABLES

NOMENCLATURE

$a,\ a_n$	=	constants used in solution of heat equation (no losses), Section II, K
a	=	constant used in solution of slug heat-balance equation (with losses), Section III, K/s
A	=	frontal area of slug = cross-sectional area, m^2
A	=	one of the constants in the Shomate equation
b	=	constant used in solution of slug heat-balance equation (with losses), Section III, s^{-1}
$c_p(T)$	=	heat capacity when it is a function of T with the Shomate equation, J/kg K
c_p	=	heat capacity of slug, J/kg K
c_{po}	=	heat capacity of slug at T_o, J/kg K
D	=	diameter of slug, m
$FracLoss$	=	the fraction of q that is a loss
$g(x)$	=	$w(x,0)$, to emphasize it is a function of x only
h	=	heat-transfer coefficient for surface regions of FEA model, Section V, W/m^2 K
k	=	thermal conductivity of slug, W/m K
L	=	length of slug, m
M	=	mass of slug, kg
n	=	series of positive integers, 1, 2, 3…
q	=	q_{input}, constant heat flux applied to front face of slug starting at $t = 0$, W/m^2
$q_{indicated}$	=	heat flux inferred at back face of slug by equation (2.29), W/m^2
q_{loss}	=	heat flux loss per unit frontal area of slug, W/m^2
$q_{slopeTave}$	=	heat flux based on the temperature-time slope and heat capacity of T_{ave}, W/m^2
$q_{slopeTb}$	=	heat flux based on the temperature-time slope and heat capacity of T_b, W/m^2
R_l	=	actual loss resistance, K/W
R_{la}	=	apparent loss resistance, K/W
$T(x,t)$	=	temperature of slug as a function of x and t, K
T	=	temperature, K
t	=	time, s
t_o	=	time when perfect step function "q on" would have occurred, equation (3.12)
t_1	=	time defining lower end of range over which T_b vs. t data are fit to equation (3.7)
t_2	=	time defining upper end of range over which T_b vs. t data are fit to equation (3.7)

NOMENCLATURE (cont.)

$t_{c\ in}$	=	time when the slug has just reached the point of heat-flux measurement (i.e., at nozzle centerline for arc jets)
$t_{c\ out}$	=	time just preceding when the slug begins to leave the point of heat-flux measurement
T_{ave}	=	average temperature of slug, K
T_b	=	back-face temperature of slug, K
T_{b1fit}	=	T of back face corresponding to time t_1 according to the best fit of equation (3.7)
T_f	=	front-face temperature of slug, K
T_o	=	uniform T of slug prior to start of application of constant heat flux q at $t = 0$, K
t_p	=	heat penetration time, time for heat to penetrate to back face, s
t_R	=	slug response time, s
$t_{R0.99}$	=	t_R for 0.99 of q_{input} to be detectible at slug back face, according to equation (2.38), s
$v_{ss}(x,t)$	=	steady-state portion of solution to heat equation
$w(x,t)$	=	transient portion of solution to heat equation
x	=	position along length of slug; $x = 0$ is front face and $x = L$ is back face, m
x_c	=	alternate coordinate for position along length of slug as used in Carslaw and Jaeger text (ref. 5), where $x_c = 0$ is back face and $x_c = L$ is front face, m
α	=	thermal diffusivity of slug, m^2/s
$\theta(t)$	=	separation of variables function of t
λ	=	separation of variables constant, m^{-1}
λ_n	=	series of separation of variables constants for $n = 1, 2, 3\ldots$, m^{-1}
ρ	=	density of slug, kg/m^3
$\varphi(x)$	=	separation of variables function of x, K

THERMAL CAPACITANCE (SLUG) CALORIMETER THEORY INCLUDING HEAT LOSSES AND OTHER DECAYING PROCESSES

T. Mark Hightower,[*] Ricardo A. Olivares,[†] and Daniel Philippidis[‡]

ABSTRACT

A mathematical model, termed the Slug Loss Model, has been developed for describing thermal capacitance (slug) calorimeter behavior when heat losses and other decaying processes are not negligible, where the temperature time slope decreases noticeably with time. This model is derived from heat-transfer and energy-balance principles along with some simplifying assumptions, and results in the temperature time slope taking the mathematical form of exponential decay. When data are found to fit well to this model, a heat-flux value can be calculated that corrects for the losses and may be a better estimate of the cold-wall fully catalytic heat flux, as is desired in arc-jet testing.

The model was applied to the data from a copper (oxygen-free high-conductivity (OFHC)) slug calorimeter inserted during a particularly severe high-heating-rate arc jet run to illustrate its use. The Slug Loss Model gave a cold-wall heat flux 15% higher than the value of 2,250 W/cm^2 obtained from the conventional approach to processing the data (where no correction is made for losses). For comparison, a Finite Element Analysis (FEA) model was created using the commercial software program COMSOL Multiphysics, where conduction heat losses from the slug were simulated. Very close agreement between the temperature-versus-time result of the FEA model and the actual data was obtained by a unique solution of both the heat flux and heat-loss coefficient specified in the FEA model. A sensitivity analysis showed that this value of heat flux as determined from the FEA model was determinable to within ± 1%, and was also found to be in close agreement with the heat flux determined by the Slug Loss Model. The FEA model accounted for temperature-dependent physical properties, heat capacity with the Shomate equation, and thermal conductivity with a simple linear fit. Although this work was applied to arc-jet test applications of slug calorimeters, it should have general applicability wherever slug calorimeters are used and losses are significant. The idealized theory of slug calorimeters for no losses and constant physical properties is also developed as a necessary basis for the general derivation presented.

[*] Engineer, Thermophysics Facilities Branch, M/S 229-4, Ames Research Center, Moffett Field, CA.
[†] Engineer, Thermophysics Facilities Branch, M/S 213-8, Ames Research Center, Moffett Field, CA.
[‡] Masters Student, Department of Mechanical and Aerospace Engineering, San Jose State University, San Jose, CA.

I. INTRODUCTION

A slug calorimeter determines heat flux by measuring the rate at which a slug of material heats up while subjected to a heat source. Arc jets are ground test facilities that are used to produce heating and flow environments similar to those experienced in planetary atmospheric entry in order to test spacecraft thermal protection materials and systems. Slug calorimeters are used for calibration of arc-jet test conditions (ref. 1). For arc-jet applications the slug is usually made of oxygen-free high-conductivity (OFHC) copper. Figure 1 shows an assembly drawing of an arc-jet slug calorimeter.

Heat losses from the slug to its holder are of concern, and are difficult to control under high-heat-flux conditions (ref. 2). The American Society for Testing and Materials (ASTM) standard (ref. 1) recommends using the slug cool-down slope after removal from the heat source as an indication of the losses during the heating phase. This approach assumes that the conditions causing the losses are the same whether subjected to or removed from the heat source—an assumption that evidence suggests is not always valid. The ASTM standard also recommends that these losses be less than 5% of the heating rate in order to be neglected.

This current work explores how losses during the heating phase can be determined more directly based on the behavior of the temperature time slope during the heating phase, where the temperature time slope decreases more rapidly than can be explained by an increase in the heat capacity of the copper slug alone. Furthermore, this work explores how these losses can be accounted for in the computed value of heat flux. Correcting slug calorimeter results for heat losses to achieve more accuracy has been recommended in the literature (ref. 3).

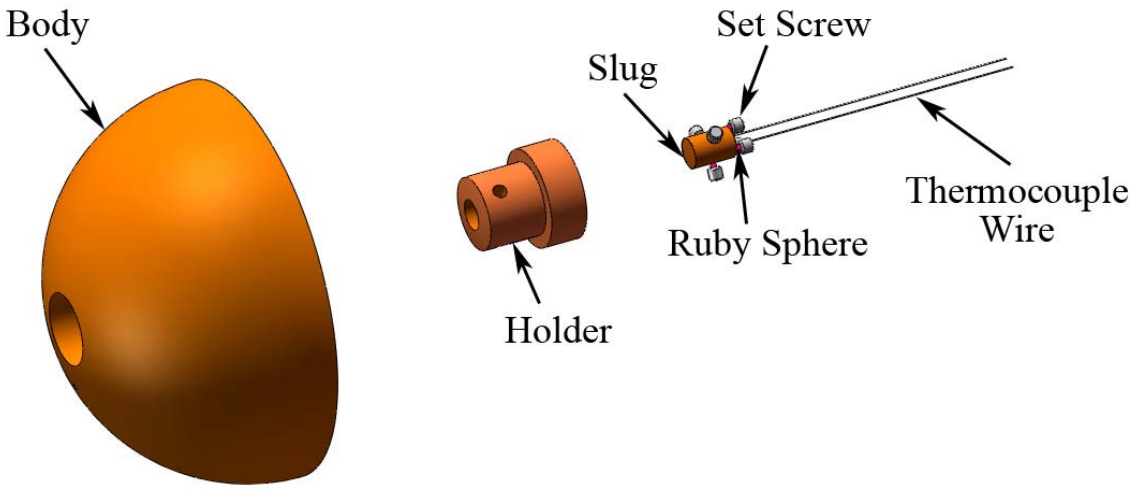

Figure 1. Assembly drawing of hemispherical slug calorimeter.

To provide the necessary groundwork, Section II covers slug calorimeter theory where no heat losses and constant physical properties are assumed. Then Section III covers slug calorimeter theory where losses and variable heat capacity with temperature are taken into account. Section IV shows in detail the application of the theory of Section III to real data from one arc-jet run, and Section V shows and compares results from a FEA model of the same run. Finally, Section VI presents conclusions.

II. NO HEAT LOSSES AND CONSTANT PHYSICAL PROPERTIES

A study in which this specific problem was fully derived was not found, although one or more must surely exist. Instead a textbook was found wherein the applicable method of solution was clearly explained, allowing for application of the method to this problem (ref. 4).

Consider a slug calorimeter, a right circular cylinder of solid OFHC copper, with diameter D and length L, initially at constant uniform temperature T_o. At $t = 0$ uniform constant heat flux q is applied at one end, the front face, while the back face and cylindrical surface are idealized to be perfectly insulated, as shown in figure 2.

Therefore, the heat flow can be modeled as one-dimensional unsteady-state heat transfer. The temperature of the slug is measured at the back face with a thermocouple. Define $x = 0$ as the front face and $x = L$ as the back face.

The one-dimensional unsteady-state heat-balance differential equation is

$$\frac{\partial^2 T}{\partial x^2} = \frac{\rho c_p}{k}\frac{\partial T}{\partial t} \tag{2.1}$$

The thermal diffusivity is defined as

$$\alpha = \frac{k}{\rho c_p} \tag{2.2}$$

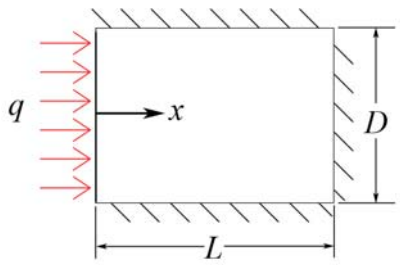

Figure 2. Boundary conditions for idealized model.

The boundary conditions are

$$\frac{\partial T(0,t)}{\partial x} = -\frac{q}{k}$$
$$\frac{\partial T(L,t)}{\partial x} = 0 \tag{2.3}$$

The initial condition is

$$T(x,0) = T_o \tag{2.4}$$

The main steps in the solution of this boundary-value problem by the method of separation of variables are outlined as follows. All physical properties are assumed to be constant.

First express the solution as the sum of two parts, the steady-state solution and the transient solution.

$$Overall\ solution = steady\text{–}state\ solution + transient\ solution$$
$$T(x,t) = v_{ss}(x,t) + w(x,t) \tag{2.5}$$

The "steady-state solution" here is the solution that applies when *t* becomes large, where the temperature everywhere in the slug is increasing at the same rate, such that

$$\frac{\partial T}{\partial t} = constant \tag{2.6}$$

The transient solution is a correction to the steady-state solution for when *t* is small, and it approaches zero as *t* becomes large. Through derivation the steady-state solution was determined to be

$$v_{ss}(x,t) = T_o + \frac{qt}{L\rho c_p} + \frac{qL}{3k} + \frac{qx^2}{2Lk} - \frac{qx}{k} \tag{2.7}$$

That this solution is correct can be verified by noting that it satisfies: the differential equation (2.1), the steady-state criterion of equation (2.6), and equation (2.8) based on an overall energy balance on the slug from $t = 0$ to $t = t$. In words this equation states that the heat added to the slug must be reflected in its average temperature.

$$T_{ave} = T_o + \frac{qt}{L\rho c_p} = \frac{1}{L}\int_0^L T dx \tag{2.8}$$

Substituting $v_{ss}(x,t)$ for T in the integral of equation (2.8) and evaluating the integral gives

$$\begin{aligned}
&\frac{1}{L}\int_0^L v_{ss}(x,t)dx = \frac{1}{L}\int_0^L \left(T_o + \frac{qt}{L\rho c_p} + \frac{qL}{3k} + \frac{qx^2}{2Lk} - \frac{qx}{k} \right) dx = \\
&\frac{1}{L}\int_0^L \left(T_o + \frac{qt}{L\rho c_p} \right) dx + \frac{1}{L}\int_0^L \left(\frac{qL}{3k} + \frac{qx^2}{2Lk} - \frac{qx}{k} \right) dx = \\
&\left(T_o + \frac{qt}{L\rho c_p} \right) + \frac{1}{L}\int_0^L \left(\frac{qL}{3k} + \frac{qx^2}{2Lk} - \frac{qx}{k} \right) dx = \\
&\left(T_o + \frac{qt}{L\rho c_p} \right) + 0
\end{aligned} \tag{2.9}$$

Applying the change of variable from T to w to the differential equation gives

$$\frac{\partial^2 w}{\partial x^2} = \frac{1}{\alpha}\frac{\partial w}{\partial t} \tag{2.10}$$

The boundary conditions in w are

$$\begin{aligned}
\frac{\partial w(0,t)}{\partial x} &= 0 \\
\frac{\partial w(L,t)}{\partial x} &= 0
\end{aligned} \tag{2.11}$$

The initial condition is

$$w(x,0) = \frac{-qx^2}{2Lk} + \frac{qx}{k} - \frac{qL}{3k} \tag{2.12}$$

It is the change of variables that allows w to be solved by the separation of variables method, because the boundary conditions in w are homogeneous. So the separation-of-variables method proposes that

$$w(x,t) = \phi(x)\theta(t) \tag{2.13}$$

Substituting into the partial differential equation produces two ordinary differential equations:

$$\begin{aligned}
&\frac{\partial^2 w}{\partial x^2} = \phi''(x)\theta(t) \\
&\frac{\partial w}{\partial t} = \phi(x)\theta'(t) \\
&\phi''(x)\theta(t) = \frac{1}{\alpha}\phi(x)\theta'(t) \\
&\frac{\phi''(x)}{\phi(x)} = \frac{1}{\alpha}\frac{\theta'(t)}{\theta(t)} = -\lambda^2 \\
&\phi'' + \lambda^2\phi = 0 \\
&\theta' + \alpha\lambda^2\theta = 0
\end{aligned} \tag{2.14}$$

The negative sign in front of λ^2 is needed because without it a trivial solution is obtained. The general solutions to these differential equations are

$$\begin{aligned}
&\phi(x) = a\cos\lambda x + b\sin\lambda x \\
&\theta(t) = e^{-\alpha\lambda^2 t}
\end{aligned} \tag{2.15}$$

The boundary conditions become

$$\begin{aligned}
&\frac{\partial w(x,t)}{\partial x} = \phi'(x)\theta(t) \\
&\frac{\partial w(0,t)}{\partial x} = \phi'(0)\theta(t) = 0 \\
&\frac{\partial w(L,t)}{\partial x} = \phi'(L)\theta(t) = 0
\end{aligned} \tag{2.16}$$

Since $\theta(t) = 0$ would give a trivial solution, the boundary conditions become

$$\begin{aligned}
&\phi'(0) = 0 \\
&\phi'(L) = 0
\end{aligned} \tag{2.17}$$

Apply the first boundary condition

$$\begin{aligned}
&\phi'(0) = 0 \\
&\phi'(x) = -a\lambda\sin\lambda x + b\lambda\cos\lambda x \\
&\phi'(0) = -a\lambda\sin(0) + b\lambda\cos(0) = 0 \\
&b = 0 \\
&\therefore \phi(x) = a\cos\lambda x
\end{aligned} \tag{2.18}$$

Apply the second boundary condition

$$\begin{aligned}\phi'(L) &= -a\lambda \sin \lambda L = 0 \\ \lambda_n &= \frac{n\pi}{L} \\ n &= 1, 2, 3...\end{aligned} \tag{2.19}$$

At this point the solution to the partial differential equation in *w* can be expressed as

$$w(x,t) = \sum_{n=1}^{\infty} a_n \cos\left(\frac{n\pi x}{L}\right) e^{-\alpha\left(\frac{n\pi}{L}\right)^2 t} \tag{2.20}$$

Now it remains to apply the initial condition in order to solve for the constants a_n.

$$w(x,0) = \sum_{n=1}^{\infty} a_n \cos\left(\frac{n\pi x}{L}\right) = \frac{-qx^2}{2Lk} + \frac{qx}{k} - \frac{qL}{3k} = g(x) \tag{2.21}$$

Equation (2.21) is a problem in Fourier series, which is solved by

$$a_n = \frac{2}{L}\int_0^L g(x)\cos\left(\frac{n\pi x}{L}\right)dx = -\frac{2qL}{k\pi^2}\frac{1}{n^2} \tag{2.22}$$

The transient solution then becomes

$$w(x,t) = -\frac{2qL}{k\pi^2}\sum_{n=1}^{\infty}\frac{1}{n^2}\cos\left(\frac{n\pi x}{L}\right)e^{-\alpha\left(\frac{n\pi}{L}\right)^2 t} \tag{2.23}$$

Finally, combining equations (2.7) and (2.23) yields the overall solution to the partial differential equation:

$$T(x,t) = \left(T_o + \frac{qt}{L\rho c_p} + \frac{qL}{3k} + \frac{qx^2}{2Lk} - \frac{qx}{k}\right) - \frac{2qL}{k\pi^2}\sum_{n=1}^{\infty}\frac{1}{n^2}\cos\left(\frac{n\pi x}{L}\right)e^{-\alpha\left(\frac{n\pi}{L}\right)^2 t} \tag{2.24}$$

Factoring out common terms and applying equation (2.2) gives

$$T(x,t) = T_o + \frac{qL}{k}\left(\frac{\alpha t}{L^2} + \frac{1}{3} + \frac{1}{2}\left(\frac{x}{L}\right)^2 - \frac{x}{L} - \frac{2}{\pi^2}\sum_{n=1}^{\infty}\frac{1}{n^2}\cos\left(\frac{n\pi x}{L}\right)e^{-\alpha\left(\frac{n\pi}{L}\right)^2 t}\right) \tag{2.25}$$

As a check on equation (2.25), it is worth comparing it to the equivalent solution given in the classic text by Carslaw and Jaeger (ref. 5). What makes comparing the solutions problematic is that their text defines the x coordinate as zero at the back face of the slug and L at the front face. So call the coordinate in the Carslaw and Jaeger text x_c to distinguish it from the x of this paper, and make a change of variable in equation (2.25) according to the following equation:

$$x = L - x_c \tag{2.26}$$

Making this change of variable and simplifying yields the following equation, which is exactly equivalent to that given in the Carslaw and Jaeger text when T_o is set equal to zero (ref. 5).

$$T(x_c,t) = T_o + \frac{qL}{k}\left(\frac{\alpha t}{L^2} - \frac{1}{6} + \frac{1}{2}\left(\frac{x_c}{L}\right)^2 - \frac{2}{\pi^2}\sum_{n=1}^{\infty}\frac{(-1)^n}{n^2}\cos\left(\frac{n\pi x_c}{L}\right)e^{-\alpha\left(\frac{n\pi}{L}\right)^2 t}\right) \tag{2.27}$$

By inspecting equation (2.25), as expected it is seen that as t increases the summation term goes to zero, and the solution becomes a parabolic temperature profile that is everywhere increasing at the same rate, that is, $\frac{\partial T(x,\infty)}{\partial t} = constant$.

$$\frac{\partial T(x,\infty)}{\partial t} = \frac{q\alpha}{kL} = \frac{q}{\rho c_p L} = \frac{qA}{Mc_p} \tag{2.28}$$

where A is the frontal area of the slug and M is its mass.

It is this behavior upon which the theory of slug calorimeter operation is based. When enough time has elapsed, the rate of change of the back-face temperature is the same as the rate of change of temperature everywhere throughout the slug, and therefore the back-face temperature captures the incident heat flux q by the following equation:

$$q = \frac{Mc_p}{A}\frac{dT_b}{dt} = L\rho c_p \frac{dT_b}{dt} \tag{2.29}$$

where T_b = the slug back-face temperature. The analytical expression for T_b is

$$T_b = T(L,t) = T_o + \frac{q\alpha t}{kL} - \frac{1}{6}\frac{qL}{k} - \frac{2qL}{k\pi^2}\sum_{n=1}^{\infty}\frac{(-1)^n}{n^2}e^{-\alpha\left(\frac{n\pi}{L}\right)^2 t} \tag{2.30}$$

The analytical expression for the front-face temperature T_f is

$$T_f = T(0,t) = T_o + \frac{q\alpha t}{kL} + \frac{1}{3}\frac{qL}{k} - \frac{2qL}{k\pi^2}\sum_{n=1}^{\infty}\frac{1}{n^2}e^{-\alpha\left(\frac{n\pi}{L}\right)^2 t} \tag{2.31}$$

The average temperature of the slug T_{ave} is given by

$$T_{ave} = T_{ave}(t) = T_o + \frac{q\alpha t}{kL} = \frac{1}{L}\int_0^L T dx \tag{2.32}$$

The following difference equations can be written:

$$\begin{aligned} T_f - T_b &= \frac{1}{2}\frac{qL}{k} - \frac{4qL}{k\pi^2}\sum_{n=1}^{\infty}\frac{1}{(2n-1)^2}e^{-\alpha\left(\frac{(2n-1)\pi}{L}\right)^2 t} \\ T_{ave} - T_b &= \frac{1}{6}\frac{qL}{k} + \frac{2qL}{k\pi^2}\sum_{n=1}^{\infty}\frac{(-1)^n}{n^2}e^{-\alpha\left(\frac{n\pi}{L}\right)^2 t} \end{aligned} \tag{2.33}$$

The summations in all of these equations approach zero as t becomes large.

It can be shown that if enough time has elapsed for the heat to have just penetrated to the backside of the slug, the summation terms are well represented by truncating the summations with the first term, for t greater than or equal to the penetration time t_p.

$$T_b = T_o + \frac{q\alpha t}{kL} - \frac{1}{6}\frac{qL}{k} + \frac{2qL}{k\pi^2}e^{-\alpha\left(\frac{\pi}{L}\right)^2 t} \tag{2.34}$$

Take the derivative and set it equal to zero to solve for t_p:

$$\begin{aligned} \frac{dT_b}{dt} &= \frac{q\alpha}{kL} - \frac{2q\alpha}{kL}e^{-\alpha\left(\frac{\pi}{L}\right)^2 t_p} = 0 \\ t_p &= \frac{L^2}{\alpha\pi^2}\ln(2) \end{aligned} \tag{2.35}$$

Now do a more general treatment for response time t_R. Make a distinction between q_{input} to the front face and $q_{indicated}$ based on the slug calorimeter equation applied at the back face.

$$\begin{aligned} q &= q_{input} \\ q_{indicated} &= L\rho c_p \frac{dT_b}{dt} \\ \frac{q_{indicated}}{q_{input}} &= \frac{\left(L\rho c_p \frac{dT_b}{dt}\right)}{q_{input}} = \frac{\rho c_p \alpha}{k} - \frac{2\rho c_p \alpha}{k}e^{-\alpha\left(\frac{\pi}{L}\right)^2 t} = 1 - 2e^{-\alpha\left(\frac{\pi}{L}\right)^2 t_R} \end{aligned} \tag{2.36}$$

$$t_R = \frac{L^2}{\alpha\pi^2} \ln\left(\frac{2}{1 - \frac{q_{indicated}}{q_{input}}} \right) \tag{2.37}$$

For practical purposes, the response time calculated when $\frac{q_{indicated}}{q_{input}} = 0.99$ should be sufficient elapsed time for the heat-flux determination from the back-face temperature to begin to be valid.

$$t_{R0.99} = \frac{L^2}{\alpha\pi^2} \ln\left(\frac{2}{1 - 0.99} \right) \tag{2.38}$$

In the next section this value $t_{R0.99}$ is used as the response time necessary to ensure that the slug has reached steady state, where the temperature profile has established its parabolic shape.

III. HEAT LOSSES AND VARIABLE HEAT CAPACITY – SLUG LOSS MODEL

In this section the theory is developed to handle the case of slug calorimeters where heat losses from slug to surroundings (as well as other possible decaying processes) are taken into account. This theory is developed in order to create a model to fit to real data, where losses are often evident by a *T*-versus-*t* slope that decreases with time more than can be accounted for by the increasing heat capacity of the copper slug with temperature alone.

A heat balance on the slug with losses gives

$$input - output(i.e.\ losses) = accumulation$$

$$qA - \frac{\left(T_{ave} - T_o\right)}{R_{la}} = Mc_{po} \frac{dT_{ave}}{dt} \tag{3.1}$$

The surroundings (slug holder) to which the slug loses heat is assumed to be at the same temperature as the initial temperature of the slug, T_o, and this surrounding temperature is assumed to remain constant. R_{la} is defined as the apparent resistance to heat loss, which is coupled with c_{po}, the constant value of c_p at temperature T_o. These parameters are coupled so that equation (3.1) can be analytically integrated. Later the actual resistance to heat loss, R_l, will be solved for when heat capacity as a function of temperature, $c_p(T_{ave})$, is introduced. At this point the effect of increasing c_p with temperature is accounted for as an additional apparent loss incorporated into the value of R_{la}.

It is desired to get equation (3.1) in terms of T_b, the temperature that is recorded as data. Assume that enough time has elapsed so that the parabolic temperature profile through the slug has been established, a condition that should be the case for $t > t_{R0.99}$ from equation (2.38). From equation (2.33) for $t > t_{R0.99}$, the summation drops out as zero and gives

$$T_{ave} - T_b = \frac{qL}{6k} \tag{3.2}$$

Solving this equation for T_{ave} gives

$$T_{ave} = T_b + \frac{qL}{6k} \tag{3.3}$$

Substituting this result into equation (3.1) gives

$$\left(q\left(\frac{A}{Mc_{po}} - \frac{L}{6kR_{la}Mc_{po}} \right) + \frac{T_o}{R_{la}Mc_{po}} \right) - \frac{T_b}{R_{la}Mc_{po}} = \frac{dT_b}{dt} \tag{3.4}$$

Define two constants:

$$\begin{aligned} a &= \left(q\left(\frac{A}{Mc_{po}} - \frac{L}{6kR_{la}Mc_{po}} \right) + \frac{T_o}{R_{la}Mc_{po}} \right) \\ b &= \frac{1}{R_{la}Mc_{po}} \end{aligned} \tag{3.5}$$

Now equation (3.4) can be written as:

$$a - bT_b = \frac{dT_b}{dt} \tag{3.6}$$

This equation integrates to

$$T_b = \left(T_{b1\,fit} - \frac{a}{b} \right) e^{-b(t-t_1)} + \frac{a}{b} \tag{3.7}$$

This equation can be used to fit actual slug calorimeter data recorded during an arc-jet run by taking the following steps:

First determine the time when the slug arrived at the position where the heat flux is to be measured. Then add $t_{R0.99}$ from equation (2.38) to this time to get t_1, the initial time for which the data will be processed. This step ensures that steady state has been reached by time t_1. Next, determine t_2, the final time for which the data will be processed, by taking the time just before the slug begins to be

removed from the heat source. Now there is a range of T_b-versus-t data points from t_1 to t_2 to fit with equation (3.7). (If the slug has been left exposed to the heat source longer than is necessary, an alternate approach might also be used to select t_2. In such a case, adding $t_{R0.99}$ or perhaps 1.5 times $t_{R0.99}$ to t_1 to get t_2 might be a better approach. This approach would help ensure the validity of the assumption of constant surrounding temperature T_o up to the value of t_2 where the model is being applied.)

Next assume a value of "b" and plot T_b versus $e^{-b(t-t_1)}$, which should be linear according to the equation. Next determine the value of "b" that gives the best linear fit. This determination can be made by solving for "b" that maximizes the R^2 value (coefficient of determination) for the fit. Now that "b" is known, "a" can be solved for from the intercept of the fit. Finally, T_{b1fit} can be solved for from the slope of the fit. The model equation fit to the data is now complete and ready to be compared to the data.

After the data are processed and "a" and "b" have been determined, q can be solved for by solving equation (3.5) for q:

$$q = \frac{a - bT_o}{\left(\frac{A}{Mc_{po}} - \frac{L}{6kR_{la}Mc_{po}}\right)} = \frac{Mc_{po}}{A}\frac{\left(a - bT_o\right)}{\left(1 - \frac{L}{6kR_{la}A}\right)} \tag{3.8}$$

An alternate but equivalent equation for q is

$$q = \frac{Mc_{po}}{A}\left(a - b\left(T_o - \frac{qL}{6k}\right)\right) \tag{3.9}$$

Take equation (3.7) and go back in time to t_o, the theoretical time when the step function of "q on" would have occurred had it been a perfect step function. This process goes back in time while keeping the temperature profile of the slug at steady-state. It is an idealization that differs from the actual behavior, but whether idealized or actual, the energy that heats up the slug from t_o to t_1 is the same. At $t = t_o$, $T_{ave} = T_o$. According to equation (3.2)

$$T_b(t_o) = T_o - \frac{qL}{6k} \tag{3.10}$$

When going back in time while maintaining a steady-state parabolic temperature profile, the temperature at the back face at t_o has to be less than T_o so that $T_{ave} = T_o$. Substituting equation (3.10) into equation (3.7) gives

$$T_b(t_o) = T_o - \frac{qL}{6k} = \left(T_{b1fit} - \frac{a}{b}\right)e^{-b(t_o - t_1)} + \frac{a}{b} \tag{3.11}$$

Solving this equation for t_o gives

$$t_o = t_1 - \frac{1}{b}\ln\left(\frac{T_o - \frac{qL}{6k} - \frac{a}{b}}{T_{b1fit} - \frac{a}{b}}\right) \tag{3.12}$$

Equation (3.7) gives T_b as an analytical function of time, which can be written as $T_b(t)$ to make the t functionality explicit. By using the linear relationship between T_{ave} and T_b of equation (3.3), T_{ave} can now also be expressed as an analytical function of time, $T_{ave}(t)$.

$$T_{ave}(t) = \left(\left(T_{b1fit} - \frac{a}{b}\right)e^{-b(t-t_1)} + \frac{a}{b}\right) + \frac{qL}{6k} \tag{3.13}$$

The derivative of $T_{ave}(t)$ with respect to time can also be taken analytically:

$$\frac{dT_{ave}(t)}{dt} = -b\left(T_{b1fit} - \frac{a}{b}\right)e^{-b(t-t_1)} \tag{3.14}$$

Now c_p can be introduced as a function of T_{ave} into the differential equation (3.1) as well as the actual loss resistance, R_l.

$$qA - \frac{\left(T_{ave}(t) - T_o\right)}{R_l} = Mc_p(T_{ave}(t))\frac{dT_{ave}(t)}{dt} \tag{3.15}$$

This equation can now be solved for R_l as a function of time:

$$R_l(t) = \frac{\left(T_{ave}(t) - T_o\right)}{\left(qA - Mc_p(T_{ave}(t))\frac{dT_{ave}(t)}{dt}\right)} \tag{3.16}$$

It remains to express c_p for copper as a function of T_{ave} by the Shomate equation.

$$c_p(T_{ave}) = A + BT_{ave} + CT_{ave}{}^2 + DT_{ave}{}^3 + \frac{E}{T_{ave}{}^2}$$

where

$$A = 2.789933x10^2\,\frac{J}{kgK} \qquad B = 4.421789x10^{-1}\,\frac{J}{kgK^2} \tag{3.17}$$

$$C = -4.918152x10^{-4}\,\frac{J}{kgK^3} \qquad D = 2.19879x10^{-7}\,\frac{J}{kgK^4}$$

$$E = 1.079706x10^6\,\frac{JK}{kg}$$

The Shomate equation is available at the National Institute of Standards and Technology (NIST) web site (ref. 6). The equation given by NIST was modified to get the temperature units as shown in equation (3.17), and to get it on a mass basis rather than a mole basis, the conversion of the atomic weight for copper, 63.546 g/gmole, was applied.

So now all the elements that allow the calculation of $R_l(t)$ by equation (3.16) have been assembled.

Other useful equations can also be written. Two equations can be written for heat flux based on the temperature-time slope and heat capacity, one based on T_b and the other based on T_{ave}.

$$q_{slopeTb}(t) = \frac{Mc_p(T_b(t))}{A}\frac{dT_b(t)}{dt} \tag{3.18}$$

$$q_{slopeTave}(t) = \frac{Mc_p(T_{ave}(t))}{A}\frac{dT_{ave}(t)}{dt} \tag{3.19}$$

Equation (3.18) is essentially equivalent to the current ASTM method where no correction for losses is attempted if time is chosen to be early in the steady-state region, i.e., $t = t_1$. Equation (3.19) is similar, but is probably slightly more accurate, being based on T_{ave} rather than T_b. Keep in mind that in the above equations where temperatures and derivatives of temperatures are explicitly expressed as functions of time, these functions of time all stem from the fit of the model to the data, equation (3.7).

By comparing equation (3.19) to equation (3.9), noting equations (3.10) and (3.6), recognizing that the time derivatives of T_{ave} and T_b are equal by inspection of equation (3.3), and that $T_{ave}(t_o) = T_o$, it can be shown that

$$\begin{aligned} &q = q_{slopeTave}(t_o) \\ &\frac{Mc_{po}}{A}\left(a - b\left(T_o - \frac{qL}{6k}\right)\right) = \frac{Mc_p(T_{ave}(t_o))}{A}\frac{dT_{ave}(t_o)}{dt} \\ &\frac{Mc_{po}}{A}\left(\frac{dT_b(t_o)}{dt}\right) = \frac{Mc_{po}}{A}\frac{dT_{ave}(t_o)}{dt} \end{aligned} \tag{3.20}$$

Finally, the following equations can be written for heat-flux loss and fraction loss as functions of time:

$$q_{loss}(t) = q - q_{slopeTave}(t) = q - \frac{Mc_p(T_{ave}(t))}{A}\frac{dT_{ave}(t)}{dt} \tag{3.21}$$

$$FracLoss(t) = 1 - \frac{Mc_p(T_{ave}(t))}{qA}\frac{dT_{ave}(t)}{dt} \tag{3.22}$$

Although the method developed in this section is based on the assumption of heat losses, resulting in exponential decay of the temperature time slope, the possibility that other phenomena might mimic exponential decay should not be dismissed. For example, the front surface of the slug might start out being fully catalytic, but become less so very rapidly upon insertion into the hot oxidizing plasma flow as to result in a decaying net heat flux to the slug. Under such a scenario the Slug Loss Model developed here would still provide some correction for these "losses." The next section presents the application of this model for including losses to the data from one run.

IV. ANALYSIS OF DATA FROM RUN IHF187R025

Figure 3 shows a plot of the data, where the slug back-face temperature and stagnation pressure are plotted as functions of time. The stagnation pressure is used in this run to determine when the slug reached centerline and when it left centerline, in order to be able to select the data to be processed according to the method.

Careful analysis of the stagnation pressure data shown in the figure indicates that $t_{c\ in}$ and $t_{c\ out}$ are 325.992 s and 327.102 s, respectively, where $t_{c\ in}$ is the time when the slug has just reached centerline and $t_{c\ out}$ is the time just before the slug starts to leave the centerline. T_o is determined from these data to be 302.35 K.

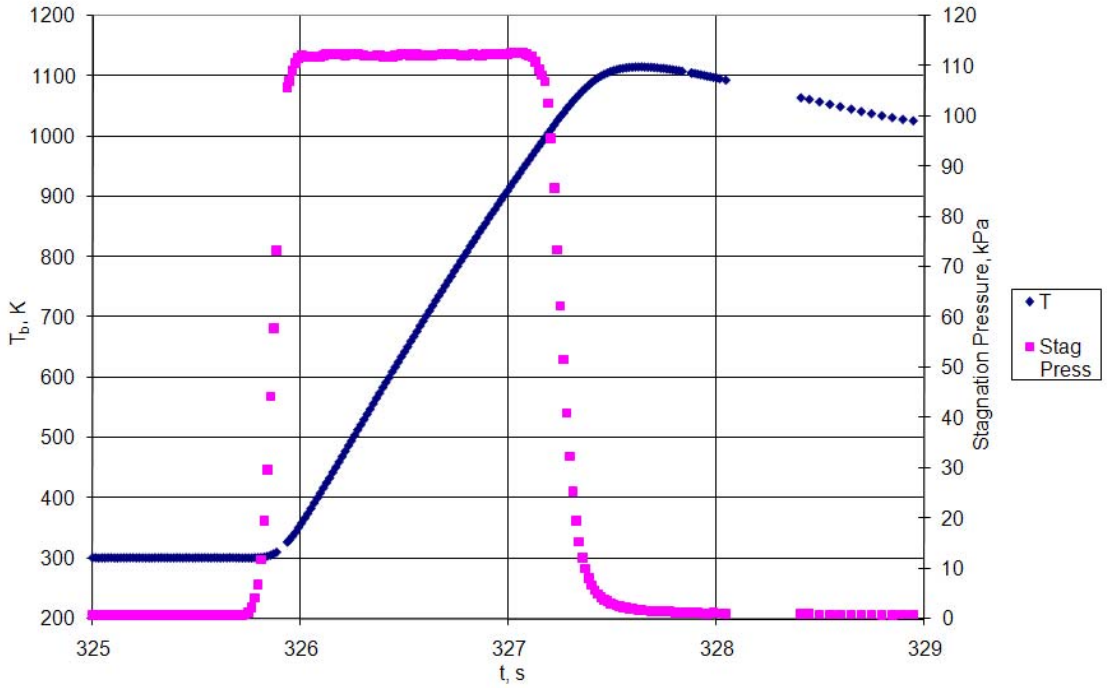

Figure 3. Back-face temperature and stagnation pressure versus time.

The physical properties of the copper slug are:

Density at 298 K, assumed a constant throughout calculations:

$$\rho = 8,925.7 \frac{kg}{m^3} \tag{4.1}$$

Thermal conductivity at 298 K, assumed a constant throughout calculations:

$$k = 385.2 \frac{W}{mK} \tag{4.2}$$

Heat capacity calculated by the Shomate equation (3.17) at T_o:

$$c_{po} = 385.615 \frac{J}{kgK} \tag{4.3}$$

Other data for the slug follow:

$$D = 0.00781\, m \tag{4.4}$$

$$M = 0.004529\, kg \tag{4.5}$$

$$A = 0.25 \pi D^2 = 0.000047906\, m^2 \tag{4.6}$$

$$L = \frac{M}{\rho A} = 0.010592\, m \tag{4.7}$$

Combining equations (2.2) and (2.38), setting $c_p = c_{po}$, and substituting for these defined values gives

$$t_{R0.99} = \frac{\rho c_{po} L^2}{k\pi^2} \ln\left(\frac{2}{1-0.99}\right) = 0.538\, s \tag{4.8}$$

Add the value of $t_{R0.99}$ to $t_{c\ in}$ to get t_1 = 326.53 s, which defines the lower end of the time span for which the data will be processed. The closest value to this in the data turns out to be t_1 = 326.532 s. The upper end of the time span, t_2, is simply equal to $t_{c\ out}$ = 327.102 s. With t_1 and t_2 defined, the data to process are shown in table 1. The data-acquisition sampling rate was about 67 data points per second.

TABLE 1. BACK-FACE TEMPERATURE VERSUS TIME DATA FROM t_1 TO t_2

t, s	Tb, K	t, s	Tb, K	t, s	Tb, K	t, s	Tb, K
326.532	660.7955	326.682	744.1884	326.832	825.295	326.983	903.1487
326.547	668.8717	326.697	752.7801	326.847	833.1806	326.997	909.7945
326.562	677.0599	326.712	760.8678	326.862	841.5302	327.012	917.442
326.577	686.4049	326.727	768.6463	326.877	848.8967	327.027	925.1961
326.592	694.5348	326.742	777.3664	326.892	856.1385	327.042	932.1872
326.608	703.5074	326.757	785.3169	326.907	864.8431	327.057	939.6873
326.622	711.217	326.773	794.0334	326.922	872.3267	327.072	947.399
326.637	719.5663	326.787	801.3908	326.937	879.3349	327.087	954.5518
326.652	728.1516	326.802	809.1195	326.952	887.2804	327.102	961.6053
326.667	736.1388	326.818	818.2387	326.967	895.0791		

Fitting this data to equation (3.7) gives the best linear fit to T_b versus $e^{-b(t-t_1)}$ when b = 0.29160 s^{-1}, where the R^2 value of the fit is maximized at 0.99999. The Solver function in an Excel spreadsheet was used to solve for b.

When b is determined, "a" can be calculated according to the equation:

$$a = \text{intercept}\left(T_b \ vs \ e^{-b(t-t_1)}\right) b = 766.76 \frac{K}{s} \tag{4.9}$$

And T_{b1fit} can be calculated according to the equation:

$$T_{b1fit} = \text{slope}\left(T_b \ vs \ e^{-b(t-t_1)}\right) + \frac{a}{b} = 660.32 \ K \tag{4.10}$$

R_{la} can be calculated according to the equation:

$$R_{la} = \frac{1}{bMc_{po}} = 1.964 \frac{K}{W} \tag{4.11}$$

And q can be calculated according to equation (3.8):

$$q = \frac{Mc_{po}}{A} \frac{\left(a - bT_o\right)}{\left(1 - \frac{L}{6kR_{la}A}\right)} = 26,005,000 \frac{W}{m^2} = 2,600 \frac{W}{cm^2} \tag{4.12}$$

This value is about 15% higher than the value of 2,250 W/cm^2 reported by the facility test engineers, where losses were not taken into account.

And t_o can be calculated according to equation (3.12):

$$t_o = t_1 - \frac{1}{b}\ln\left(\frac{T_o - \frac{qL}{6k} - \frac{a}{b}}{T_{b1\,fit} - \frac{a}{b}}\right) = 325.792\ s \tag{4.13}$$

The fictitious $T_b(t_o)$ of equation (3.10) can be calculated:

$$T_b(t_o) = T_o - \frac{qL}{6k} = 183\ K \tag{4.14}$$

The plot in figure 4 shows how the model fits the data.

Notice how the fit is extremely good, with error of fit to data of ± 0.07%. Also note that the fit is clearly not linear; this fact is easily seen by holding a straight edge to it. Figure 5 shows a plot of the losses versus time as determined from equations (3.21) and (3.22).

Notice how at t_1, the earliest point at which the slope would be eligible to be used with the current ASTM method (without corrections for losses), the losses are greater than 10%. And the losses only get larger with time.

For comparison, in the test engineer's report for this run, a heat loss of 345.4 W/cm^2 was reported during the cooling phase, after the slug was removed from the flow.

Figure 6 shows a plot of the actual loss resistance, R_l, versus t, calculated according to equation (3.16).

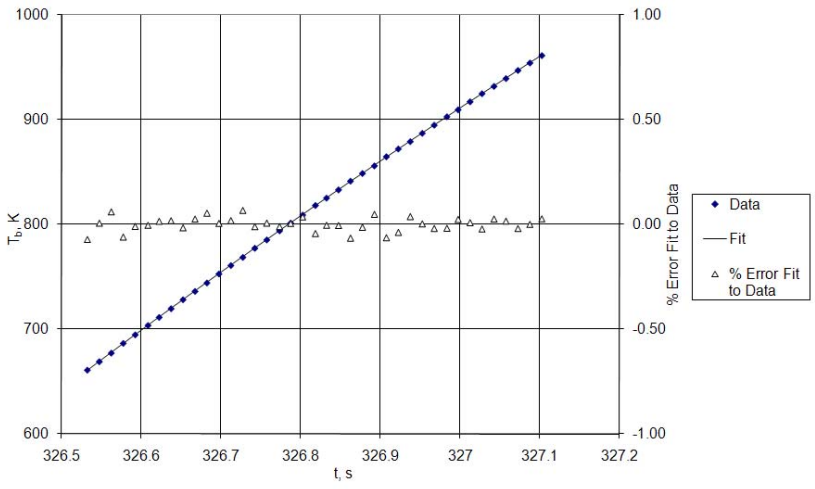

Figure 4. Back-face temperature – fit compared to data.

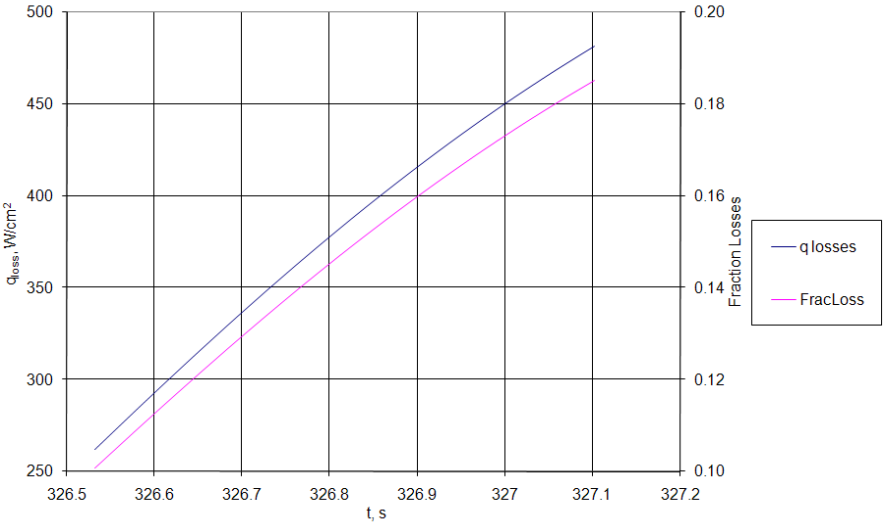

Figure 5. Losses (per cm^2 slug frontal area) versus time.

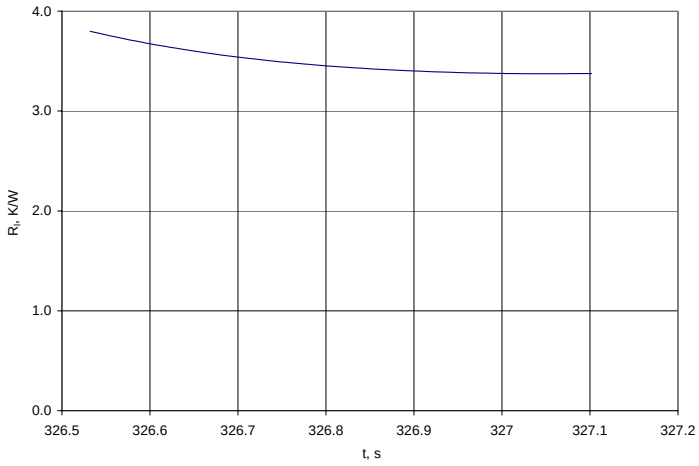

Figure 6. Actual loss resistance versus time.

V. FINITE ELEMENT ANALYSIS MODEL

A Finite Element Analysis (FEA) model was created using the commercial software program COMSOL Multiphysics, COMSOL, Inc, Burlington, Massachusetts, USA. The slug was modeled using three-dimensional (3-D) tetrahedral elements. Figure 7 shows the mesh.

The heat-loss routes from slug to holder for this model were defined as follows (reference to figure 1 is helpful for understanding this description): The actual slug is isolated from its holder by six ruby spheres of 1.5875-mm diameter, three arranged equally spaced around a concentric circle at the back side of the slug, and three arranged equally spaced around the circumference of the slug about midway from front to back. Based on measurements of pronounced dimpling observed on a slug, from the ruby spheres being forced into the copper surface of the slug during use, it was estimated that the area of contact between each ruby sphere and the slug could be represented as a circular area with diameter of 0.6 mm.

Therefore, for the FEA model, the surface areas of the slug that make contact with the ruby spheres were modeled as 0.6-mm-diameter surface regions, with a heat-transfer coefficient of h rejecting heat to a temperature of T_o, the initial temperature of the slug and assumed constant temperature of its holder. These features of the model are shown in figure 8. Note that for the purposes of this model possible heat losses through the air gap between slug and holder via convection and radiation were not considered.

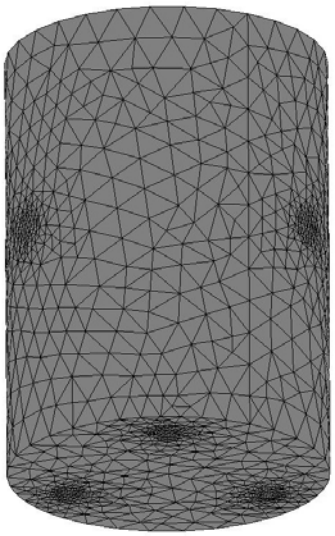

Figure 7. Model mesh.

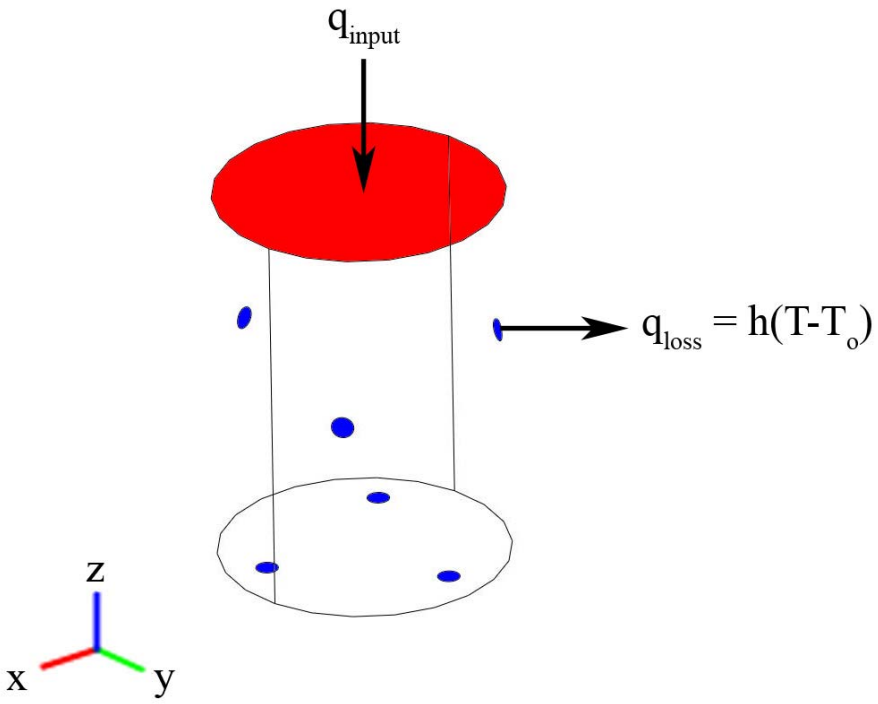

Figure 8. Boundary conditions showing the locations of the entering and exiting heat fluxes in the model.

The slug has the material properties of copper. The heat capacity varies with temperature according to the Shomate equation (3.17). Thermal conductivity (ref. 7) was fit to a linear equation (5.1).

$$k = c_1 T + c_2$$
$$c_1 = -0.071098 \frac{W}{m K^2} \tag{5.1}$$
$$c_2 = 422.915 \frac{W}{m K}$$

A smoothed Heaviside function (flc2hs from the COMSOL Library) was used to create ramp-up and ramp-down times for the heat flux applied to the front face of the model. The total simulation time of the model is 3 seconds, with a 0.01-second time step. Figure 9 shows a temperature fringe plot at the end of a run (at time t = 3 seconds).

Runs were made with the model for various values of q_{input}, h, and duration of heat pulse, until a very close agreement with the actual data was obtained with a value of q_{input} = 2,600 W/cm^2. Figure 10 shows T_b versus t for both this COMSOL solution and the actual data, where the curves lie almost exactly on top of one another, and figure 11 compares the q values as calculated from the slug calorimeter equation applied to the back face, i.e., per equation (3.18) as applied numerically to the data.

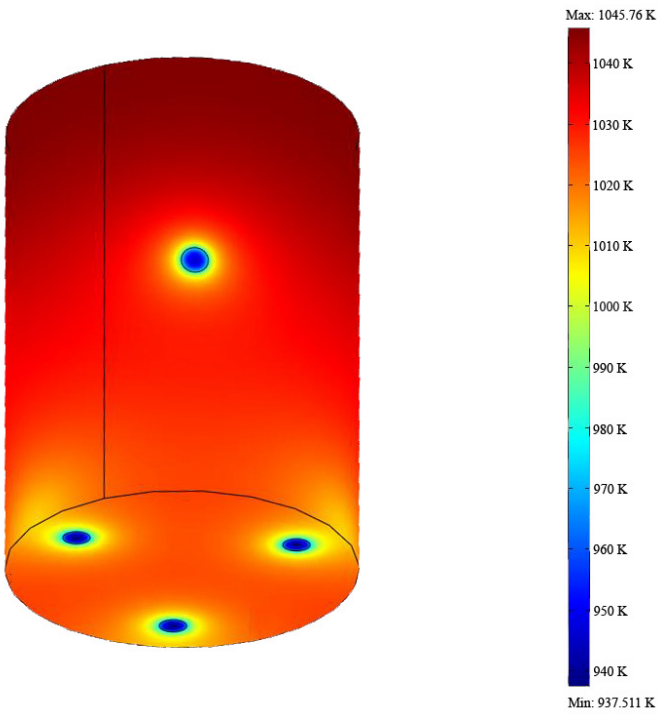

Figure 9. Temperature fringe plot of the model at time t = 3 seconds.

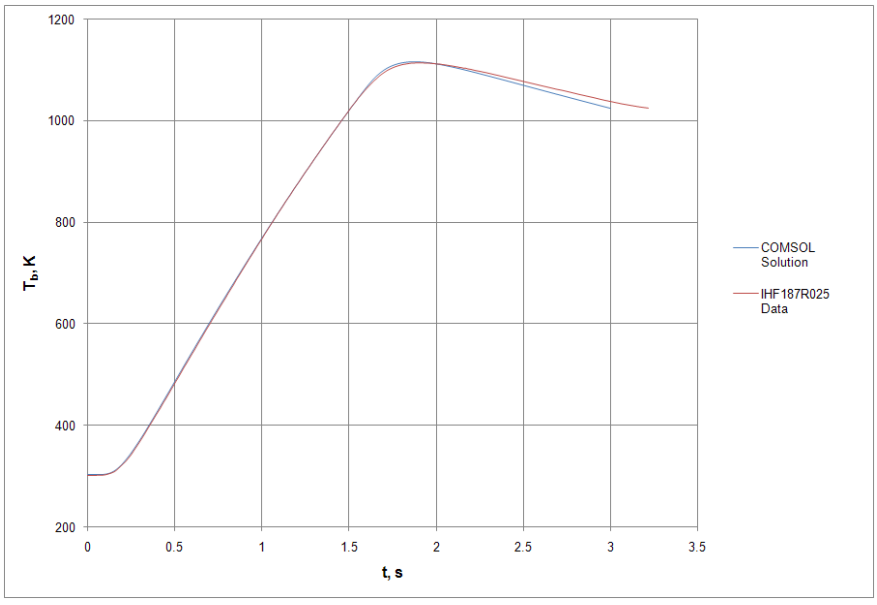

Figure 10. T_b vs. t – COMSOL model and actual data compared.

The best fit of the model to the data is obtained with a unique combination of q and h. A sensitivity analysis showed that the values of q and h so determined are known to about ± 1% and ± 10%, respectively. The temperatures of the front and back faces were plotted as a function of time; they are shown in figure 12.

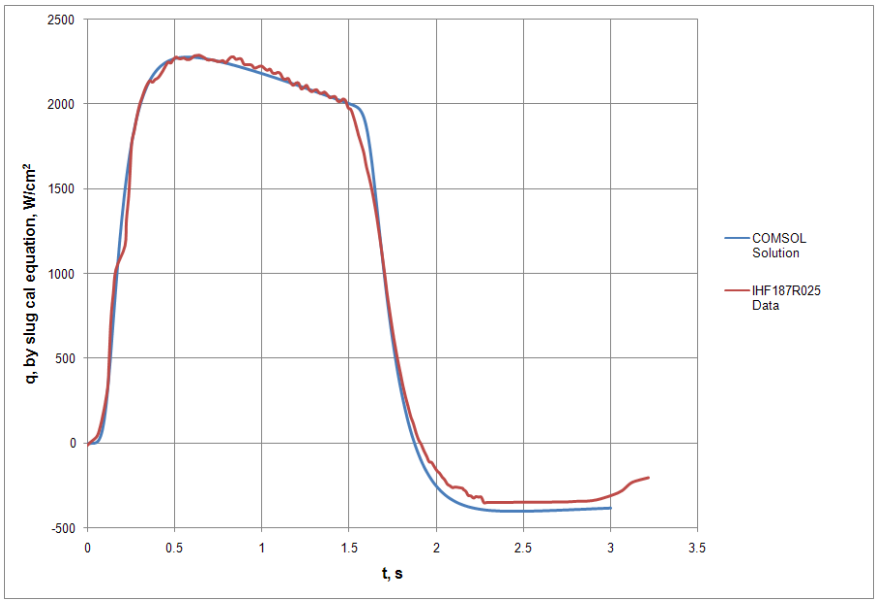

Figure 11. q versus t – COMSOL model and actual data compared.

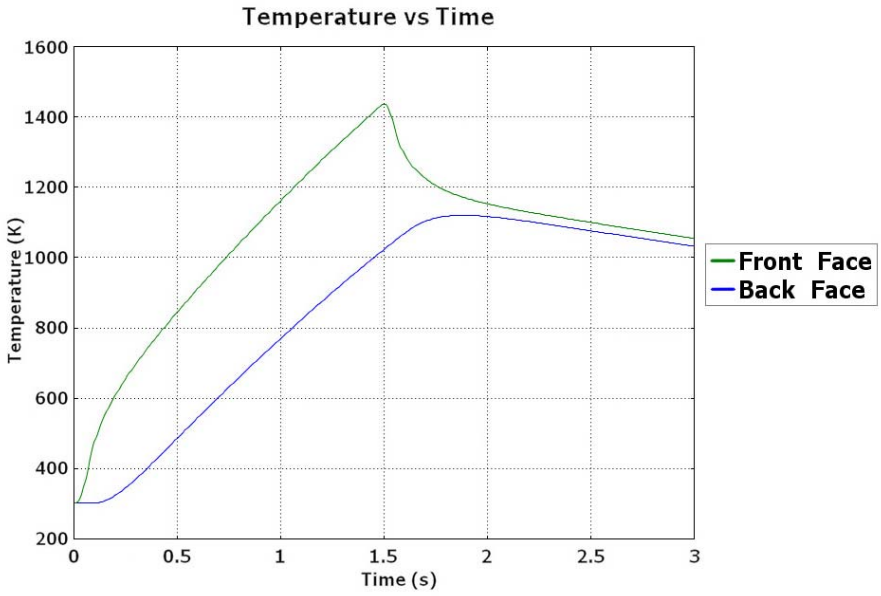

Figure 12. Temperature vs. time plots for the center of the front and back faces.

Alternate COMSOL models were used that were axisymmetric (2-D) where the ruby sphere contacts were modeled as thin concentric rings of contact area. These models gave essentially the same results as the 3-D model already presented, but had the advantage of running much faster. In the data presented in the following discussion, the COMSOL models are all based on the 2-D models, but the results would be expected to be nearly identical if the more time-consuming equivalent 3-D models were run.

COMSOL model runs were done for the following four cases: no losses and constant physical properties, no losses and variable physical properties, losses and constant physical properties, and losses and variable physical properties (the 2-D version of the 3-D case already presented). In addition, the ideal partial differential equation solution of equation (2.30) was calculated. These five cases were all based on a q_{input} value of 2,600 W/cm^2. Finally, the Slug Loss Model fit of equation (3.7) was calculated based upon the COMSOL data for the "losses and variable physical properties" case. Figure 13 compares all six of these cases.

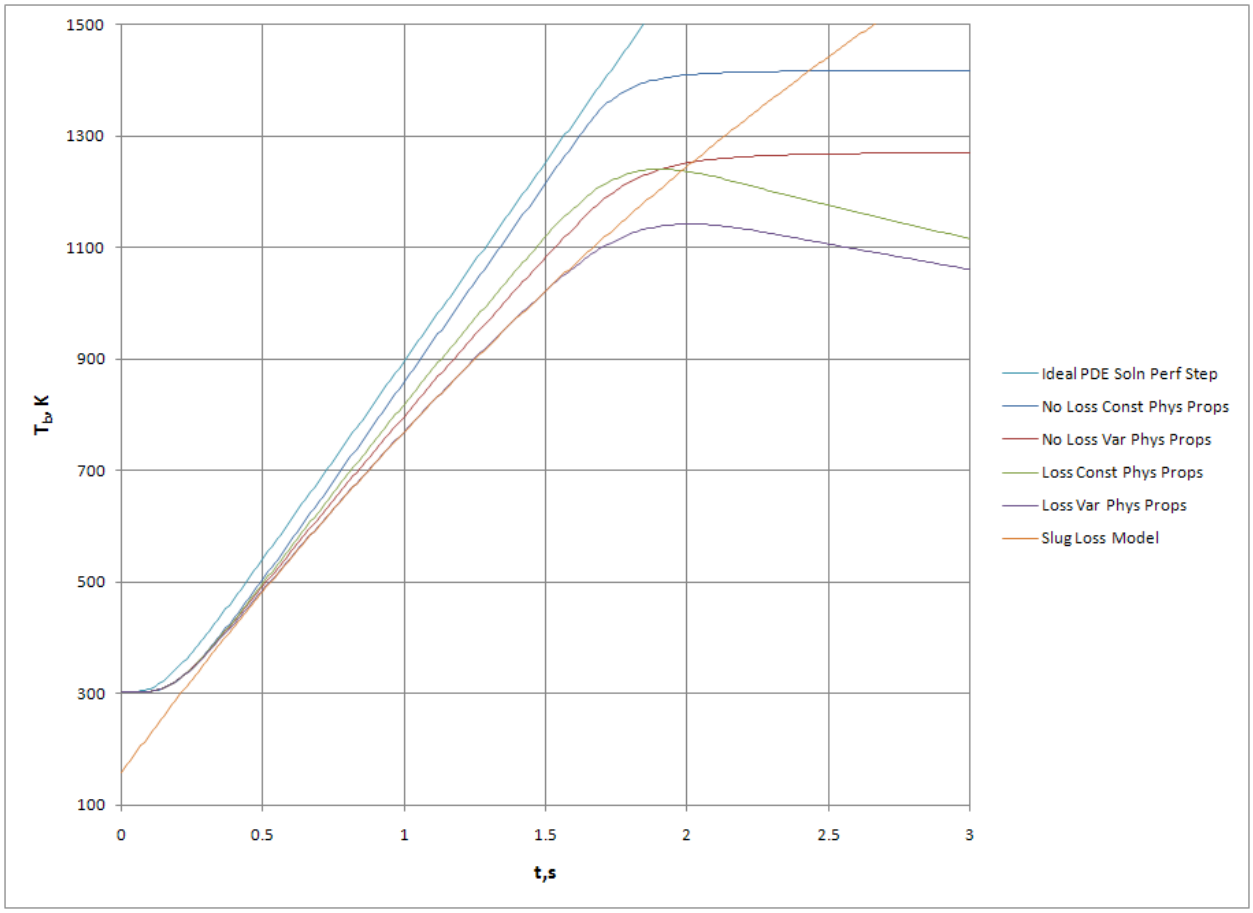

Figure 13. Results of all models compared.

The ideal partial differential equation solution has a perfect step function, so its initial transient solution is quicker than the "no losses and constant physical properties" COMSOL case that has a smoothed step function, but as expected, these two solutions parallel each other beyond the transient.

The "no losses and variable physical properties" case shows more deviation from the ideal case than the "losses and constant physical properties" case, showing that variable heat capacity contributes more to the dropping slope during the heating phase than the losses do.

The Slug Loss Model solution fit the "losses and variable physical properties" COMSOL case over the steady-state region, from t = 0.76 s to 1.3 s, the region over which the lengthwise temperature profile is roughly parabolic. As expected, the Slug Loss Model gives a value of $T_b(t_o)$ less than T_o according to equation (3.10), where t_o calculates to be about 0.04 s according to equation (3.12).

When the Slug Loss Model was run on the data from the "losses and variable physical properties" COMSOL case, it gave a q of 2,465 W/cm^2, about 5% less than the 2,600 W/cm^2 value that was determined from both the Slug Loss Model applied to the actual data and the COMSOL fit to the actual data. The reason for this difference appears to be evident in figure 11. The downward slope of the actual data is steeper over the time interval where the Slug Loss Model was fit than the downward slope of the COMSOL model fit over the same interval. The steeper downward slope is indicative of more losses, which is inferred as a higher q by the Slug Loss Model. Thus, the Slug Loss Model appears to have a bias towards underpredicting q (i.e., not fully correcting for losses) if the data were to have perfectly followed the assumptions of the COMSOL model. Based on this finding, it is best not to apply the Slug Loss Model blindly without also looking at the data plotted in the form of q versus t as in figure 11 to be sure that the data show the basic characteristics upon which the Slug Loss Model is based.

Note that in the actual slug calorimeter data case under analysis in this paper, the front face of the slug actually melted at the end of the run. This result did not appear to have a discernable impact on the data. No attempt was made to incorporate this melting in any of the models.

VI. CONCLUSIONS

A mathematical model for determining the heat flux with a slug calorimeter with high heat losses, termed the Slug Loss Model, has been presented. For a particular high-heat-flux arc-jet run, the Slug Loss Model determined a heat flux that is 15% higher than what has been calculated using the conventional approach. It was found to be in good agreement with the FEA model, reinforcing the idea that losses are occurring. This Slug Loss Model is intended to be an additional tool in the thermal analyst's toolbox that can be applied for high losses.

REFERENCES

1. ASTM Standard E457-08: Standard Test Method for Measuring Heat-Transfer Rate Using a Thermal Capacitance (Slug) Calorimeter. Annual Book of ASTM Standards: Space Simulation; Aerospace and Aircraft; Composite Materials. vol. 15, no. 03, 2008.

2. Diller, T. E.: Advances in Heat Flux Measurements. Advances in Heat Transfer, vol. 23, Academic Press, 1993, pp. 307–311.

3. Childs, P. R. N.; Greenwood, J. R.; and Long, C. A.: Heat flux measurement techniques. Proceedings of the Institution of Mechanical Engineers. vol. 213, part C, 1999, pp. 664–665.

4. Powers, D. L.: Boundary Value Problems. 5th ed., Chap. 2. Elsevier Academic Press, New York, 2006.

5. Carslaw, H. S.; and Jaeger, J. C.: Conduction of Heat in Solids. 2nd ed. Oxford University Press, London, 1959, pp. 112–113. Equation (3).

6. NIST Chemistry WebBook, http://webbook.nist.gov, data cited as from NIST Standard Reference Database 69, June 2005.

7. Linde, D. R.: CRC Handbook of Chemistry and Physics. 81st ed., CRC Press, New York, 2000, p. 12-199.

REPORT DOCUMENTATION PAGE

Form Approved
OMB No. 0704-0188

1. REPORT DATE *(DD-MM-YYYY)*	2. REPORT TYPE	3. DATES COVERED *(From - To)*
09/23/2008	Technical Memorandum	

4. TITLE AND SUBTITLE

Thermal Capacitance (Slug) Calorimeter Theory Including Heat Losses and Other Decaying Processes

5a. CONTRACT NUMBER

5b. GRANT NUMBER

5c. PROGRAM ELEMENT NUMBER

6. AUTHOR(S)

T. Mark Hightower[1], Ricardo A. Olivares[1], and Daniel Philippidis[2]

5d. PROJECT NUMBER

5e. TASK NUMBER

5f. WORK UNIT NUMBER

WBS 999574.01.02.01.02

7. PERFORMING ORGANIZATION NAME(S) AND ADDRESS(ES)

[1]Thermophysics Facilities Branch, Ames Research Center, Moffett Field, CA 94035-1000

[2]Department of Mechanical and Aerospace Engineering, San Jose State University, San Jose, CA 95192

8. PERFORMING ORGANIZATION REPORT NUMBER

A-080019

9. SPONSORING/MONITORING AGENCY NAME(S) AND ADDRESS(ES)

National Aeronautics and Space Administration
Washington, D. C. 20546-0001

10. SPONSORING/MONITOR'S ACRONYM(S)

NASA

11. SPONSORING/MONITORING REPORT NUMBER

NASA/TM–2008-215364

12. DISTRIBUTION/AVAILABILITY STATEMENT

Unclassified—Unlimited Distribution: Nonstandard
Subject Category: 34
Availability: NASA CASI (301) 621-0390

13. SUPPLEMENTARY NOTES

Point of Contact: T. Mark Hightower, Ames Research Center, MS 229-4, Moffett Field, CA 94035-1000
(650) 604-4443

14. ABSTRACT

A mathematical model, termed the Slug Loss Model, has been developed for describing thermal capacitance (slug) calorimeter behavior when heat losses and other decaying processes are not negligible. This model results in the temperature time slope taking the mathematical form of exponential decay. When data is found to fit well to this model, it allows a heat flux value to be calculated that corrects for the losses and may be a better estimate of the cold wall fully catalytic heat flux, as is desired in arc jet testing. The model was applied to the data from a copper slug calorimeter inserted during a particularly severe high heating rate arc jet run to illustrate its use. The Slug Loss Model gave a cold wall heat flux 15% higher than the value of 2,250 W/cm^2 obtained from the conventional approach to processing the data (where no correction is made for losses). For comparison, a Finite Element Analysis (FEA) model was created and applied to the same data, where conduction heat losses from the slug were simulated. The heat flux determined by the FEA model was found to be in close agreement with the heat flux determined by the Slug Loss Model.

15. SUBJECT TERMS

Thermal capacitance calorimeter, Slug calorimeter, Arc jet, Finite element analysis, FEA, COMSOL, Heat losses

16. SECURITY CLASSIFICATION OF:			17. LIMITATION OF ABSTRACT	18. NUMBER OF PAGES	19a. NAME OF RESPONSIBLE PERSON
a. REPORT	b. ABSTRACT	c. THIS PAGE			T. Mark Hightower
Unclassified	Unclassified	Unclassified	Unclassified	34	19b. TELEPHONE *(Include area code)* (650) 604-4443